

Time-Space Domain Availability Analysis under Reliability Impairments

Thilina N. Weerasinghe, Indika A. M. Balapuwaduge, and Frank Y. Li

Abstract - Availability and reliability are two essential metrics for the design, deployment, and operation of future ultra-reliable low latency communication (URLLC) networks. Despite a vast amount of research efforts towards URLLC, very little attention has been made on the ultra-reliable communication (URC) aspect of URLLC from a dependability perspective. As an effort towards achieving *anytime and anywhere* communication, this paper consolidates a dependability theory based availability concept for individual users by taking into account reliability impairments that affect URC in *both spatial and temporal domains*. To this end, we perform per-user availability analysis by considering channel status and user mobility patterns in a Poisson Voronoi network.

keywords - URC/URLLC, per-user availability, reliability impairments, time and space domains.

D.1 Introduction

Ultra-reliable communication (URC) is an essential requirement for mission-critical and industry automation applications. To support ultra-reliable low latency communications (URLLC) to end users, the fifth generation (5G) wireless networks face various challenges. Many of these challenges for downlink transmissions are related to the reliability requirements for data and control channels [1]. Achieving URC and URLLC, with respect to reliability, requires a paradigm shift in terms of terminologies, methodology, and standards in comparison with earlier generations of wireless networks [2].

From the perspective of network operators, a standard availability metric is highly anticipated to measure the *anytime and anywhere* operation of their 5G networks as a key performance indicator. On the other hand, ensuring the accuracy of reliability and/or availability evaluation requires the capability to adopt to the changes in both time and space domains together with channel conditions. While most prior work focused on reliability or availability analysis in the time domain, we proposed dependability theory based definitions to measure network and user availability by focusing on the space domain [3] or considering both space and time domains [4]. In this letter, we consolidate the proposed URC availability definition in [4] by including factors that may degrade the reliability level of a network, known as reliability impairments (RIs) [5], into our availability analysis. When determining an actual reliability level, RIs like excessive interference, resource constraints, and system failures need to be addressed.

The contributions of this work are as follows. To illustrate the applicability of the advocated definition, we perform an analysis on the URC level experienced by an individual

user in a wireless network. In order to reflect the time and space domain significance on URC availability, a mobility pattern and time varying location of a mobile user (MU) are considered in this work. Moreover, the channel status of the associated cell is modeled as a potential RI and its impact on the overall URC availability level is calculated. Additionally, we investigate different channel selection strategies when an MU is covered by more than one cell.

D.2 Per-user Availability

The per-user availability definition presented below is targeted at an individual end user but it applies to any user [4]. In order to receive services, the user should be located within the cell coverage according to a pre-defined criterion and there should be a sufficient number of vacant channels in the network. Furthermore, the effects of RIs could impair the level of availability experienced by the user even if it is covered.

Let URC-region (UR) denote the region within which URC is achieved despite RIs and $\mathbf{U}(t)$ be the set of coordinates belonging to a UR at time t . Furthermore, denote by $p_k(t)$ the position coordinates of user k at time t . Considering whether the relationship $p_k(t) \in \mathbf{U}(t)$ is true or not, we introduce an indicator random variable $I_{p_k}(t)$ as follows,

$$I_{p_k}(t) = \begin{cases} 1, & \text{if } p_k(t) \in \mathbf{U}(t) \\ 0, & \text{otherwise.} \end{cases} \quad (\text{D.34})$$

From the theory of dependability, availability is defined as the ratio between mean up time and total time which is the sum of mean up time and mean down time. Accordingly, we propose a URC availability definition from a dependability perspective for a single mobile user, k , as follows,

$$A_k = \frac{\int_0^{t_{tot}} I_{p_k}(t) dt}{t_{tot}} \quad (\text{D.35})$$

where A_k is the defined per-user availability and t_{tot} is the total observation time which is assumed to be sufficiently large. t_{tot} can be decided based on a pre-defined criterion like travel time or a fixed observation duration. The integral of the indicator function $I_{p_k}(t)$ over time gives the accumulated time during which $p_k(t) \in \mathbf{U}(t)$. Hence, the ratio between this duration and t_{tot} represents the URC availability that user k experienced during this period of time. When user k is an MU, its location is a function of time. Moreover, $\mathbf{U}(t)$ also varies over time due to the time varying impacts of RIs over UR. Hence, (D.35) provides a general expression to calculate per-user availability, capturing both time and space domain aspects that affect URC.

D.3 System Model

In this section, we introduce the system model for per-user availability analysis based on the advocated definition.

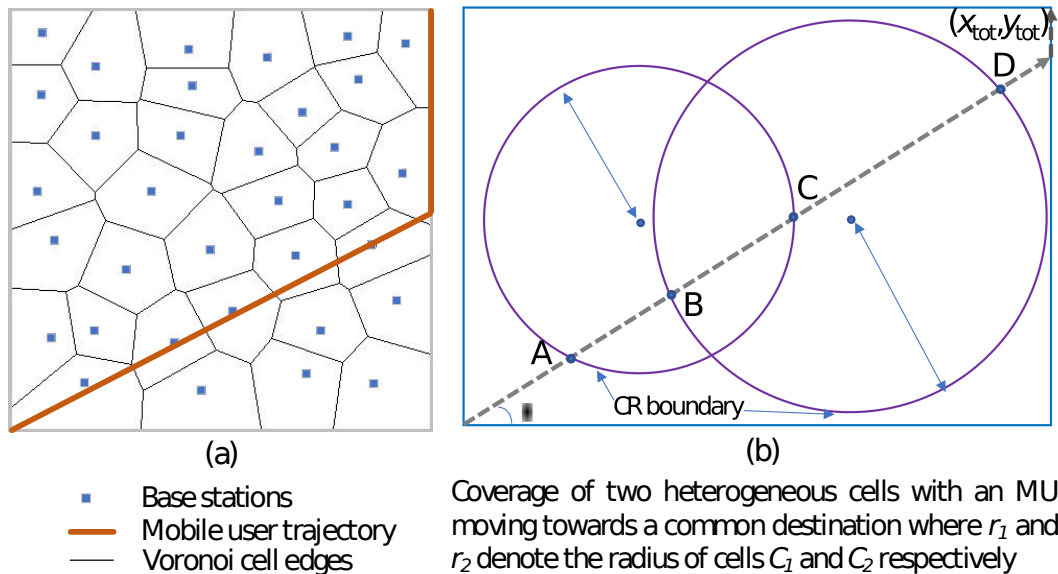


Figure D.1: (a) A PPP distributed homogeneous cellular network consisting of Voronoi cells, (b) Mobile user motion in a two-cell network.

D.3.1 Network Scenario and User Mobility

Stochastic geometry including Voronoi diagrams and Poisson point process (PPP) has been shown to be a powerful mathematical tool for modeling the random distribution of base stations (BSs) [6]. In this study, to model the cellular network with a rectangular area of interest $(x_{tot} \times y_{tot})$, a popular stochastic geometry model is adopted where the infrastructure nodes are Poisson distributed. It consists of M variable size cells forming a Voronoi tessellation. Within each cell, there is a BS located at the center of the cell with an omni-directional antenna. Moreover, a network may be deployed as a homogeneous or heterogeneous network which consists of cells with either identical or different cell sizes.

Two user mobility patterns are considered in this study, denoted as MP1 and MP2 respectively. Mobility pattern MP1 is illustrated in Fig. D.1 where the MU travels from the coordinate of origin $(0, 0)$ to its destination (x_{tot}, y_{tot}) . The MU has multiple path options to select, represented by the angle of departure, θ where $0 < \theta < \pi/2$ measured from the x -axis. If the reached boundary is not the destination, the MU will turn towards the destination at the boundary point and then move towards it either counterclockwise or clockwise. MP2 is the random direction model [7] which is a variant of the well-known random way point mobility model.

D.3.2 Cell Coverage and URC Region with RIs

For per-user availability analysis, the URC region needs to be calculated when both cell coverage and reliability impairments are considered. Let coverage-region (CR) denote the region within which the user is covered according to certain criterion. Under an ideal condition, the area of the CR for a single cell is πR^2 where R is the radius of the cell. Note however that *being covered by a BS is a necessary condition for URC provisioning but it is not sufficient.*

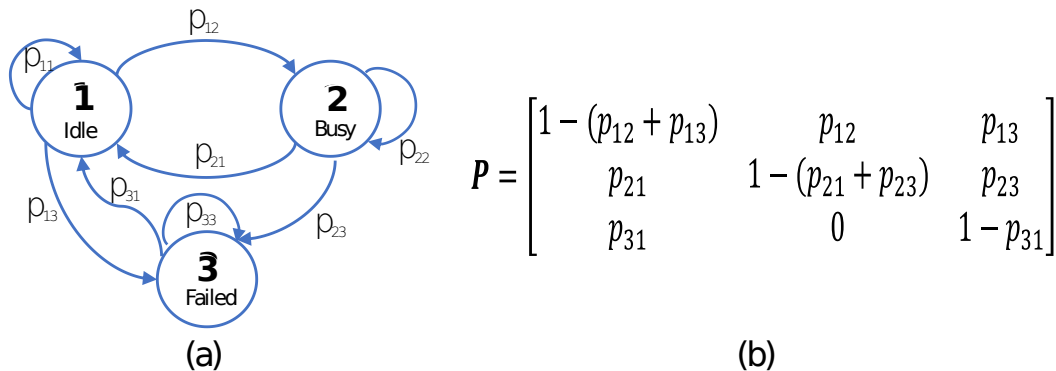


Figure D.2: (a) A DTMC with three channel states: Idle, busy, and failed; (b) Transition probability matrix of the DTMC.

D.3.3 Channel States and Channel Availability

As mentioned in Sec. D.1, resource constraints and system failures are two types of RIs that could impair URC performance. In wireless networks, channel occupancy and link status may represent such RIs. In what follows, we model error-prone channels together with channel occupancy status as examples of RI using a discrete time Markov chain (DTMC) based approach. For in-depth analysis of channel holding times and modeling of unreliable links, refer to [8] [9].

Consider that a single channel is used in each cell. To model channel status, we adopt a 3-state DTMC. Three states, **1**, **2**, and **3**, as shown in Fig. D.2(a), represent the idle, busy, and failed states of the channel respectively. The channel is considered to be idle if it is neither occupied by another user nor in a failed state. Let p_{ij} denote the transition probability from state i to state j and the steady state probability of state \mathbf{x} is denoted as $\pi_{\mathbf{x}}$. The corresponding transition probability matrix of this DTMC is presented in Fig. D.2(b).

The steady state probabilities of this DTMC can be obtained by solving the set of linear equations $\boldsymbol{\pi}\mathbf{P} = \boldsymbol{\pi}$ and $\sum_{\mathbf{x} \in \mathcal{S}} \pi_{\mathbf{x}} = 1$ where \mathcal{S} is the state space. $\boldsymbol{\pi}$ is the stationary distribution and \mathbf{P} is the transition probability matrix. A channel is regarded as available for a new MU when it is in the idle state. Otherwise, the channel is reliability impaired, i.e., when it is either in the occupied or in the failed state. Therefore, channel availability, A , for a new user can be expressed as, $A = \pi_1$.

D.4 Per-User Availability Analysis and Cell Selection Strategies

Considering that an MU is moving across multiple cells, we analyze the achieved per-user availability when channel impairments are regarded as an RI. In addition, we propose three channel selection strategies when a user is located inside a cell intersection region. By following the approach mentioned in Subsec. D.3.3, the probabilities for the three states, i.e., idle, occupied, and failed, can be obtained as $\pi_1 = p_{31}(p_{21} + p_{23}) / ((p_{31} + p_{13})(p_{21} + p_{23}) +$

$p_{12}(p_{31} + p_{23})$), $\pi_2 = \pi_1 p_{12} / (p_{21} + p_{23})$, and $\pi_3 = (\pi_1 (p_{13}(p_{21} + p_{23}) + p_{23} p_{12})) / p_{31}(p_{21} + p_{23})$, respectively.

D.4.1 Per-user Availability with RIs

Consider an arbitrarily selected MU. Its per-user availability can be obtained from (D.35). Denote by t_{in} the duration that the MU is located inside the CR. Considering the RI experienced such as channel unavailability discussed above, the per-user availability is obtained by $A_k = (t_{in}/t_{tot})\pi_1$ for a single cell.

For a multi-cell scenario, the transition probabilities vary from one cell to another. To obtain per-user availability in this case, we need to calculate the accumulated time that an MU spends in the availability state across all cells, divided by the total duration of the journey from source to destination, or the observation time. More specifically, it is given by

$$A_k = \frac{\sum_{j=1}^M t_{in}(j)\pi_1(j)}{t_{tot}}, \quad (\text{D.36})$$

where $\pi_1(j)$ denotes the steady state probability of being in the idle state of cell j , $t_{in}(j)$ denotes the duration the MU spends inside the CR of cell j during its movement. In an overlapped region across two or more cells, the MU needs to be associated with a specific cell determined by one of the strategies presented in the next subsection.

To calculate $t_{in}(j)$, $j = 1, 2, \dots, M$, the travel distance inside each cell needs to be calculated. Consider the two-cell scenario illustrated in Fig. D.1(b). The intersection points between the coverage circles of these two cells and MU's path can be calculated by substituting the center points and radius values of each cell in the places of (x_0, y_0) and r respectively and jointly solving $x = (x_0 + y_0 \tan \theta \pm \sqrt{(r^2 \sec^2 \theta) - (x_0 \tan \theta - y_0)^2}) / \sec^2 \theta$ and $y = x \tan \theta$. Once the intersection points are known, the distances between points A, B, C, and D can be obtained. Thereafter, the corresponding time values are obtained. This process can be generalized to multi-cell scenarios.

The total time t_{tot} is calculated from $t_{tot} = l_{tot}/s$, where l_{tot} is the total travel distance that can be obtained through geometric relationships [4], and s is the speed that the MU is traveling which is assumed to be constant in this study.

D.4.2 Cell Selection Strategies

When an MU enters an area where two or more cells intersect, the MU needs to take a network-assisted decision regarding which cell it will be associated with according to a specific criterion. We propose below three strategies that an MU can use for cell selection when it is covered by two or more cells, referred to as Str_1 , Str_2 , and Str_3 respectively.

- Str_1 : The cell with the highest steady state probability at the idle state will be selected.
- Str_2 : The cell with the lowest state holding time at the failed state will be selected.
- Str_3 : The cell with the lowest occupied-to-failed transition probability will be selected.

With Str_1 , the MU will compare the steady state probabilities of the overlapping cells at the idle state, i.e., $\pi_1(j)$, $j = 1, 2, \dots, M$, for each cell. Then it is associated with the

cell which has the highest π_1 . On the other hand, Str_3 is designed to give higher priority to ongoing communications. When the MU is inside an overlapped area with an ongoing session, it requires higher priority so that its ongoing communication can be completed successfully. To do so, Str_3 selects a cell which has the lowest transition probability from the busy to failed state, i.e., p_{23} .

For Str_2 , the MU selects a cell with the aim of minimizing the time spent at the failed state. To do so, a decision variable based on channel state holding times is needed. Denote by $\gamma_{\mathbf{3}}$ the number of time steps the system spent in the failed state during the visit. The distribution of the state holding time $P[\gamma_{\mathbf{3}} = h]$, where h is the number of time steps, follows a geometric distribution with parameter p_{33} . Therefore, from geometric distribution, it is known that $P[\gamma_{\mathbf{3}} = h] = (1 - p_{33})p_{33}^{h-1}$. Denote the expected value of this distribution as $E[\gamma_{\mathbf{3}}]$, then

$$\begin{aligned} E[\gamma_{\mathbf{3}}] &= \sum_{h=1}^{\infty} h(1 - p_{33})p_{33}^{h-1} = \sum_{h=1}^{\infty} \left(hp_{33}^{h-1} - hp_{33}^h \right) \\ &= \sum_{h=0}^{\infty} \left((h+1)p_{33}^h - hp_{33}^h \right) = \sum_{h=0}^{\infty} p_{33}^h = \frac{1}{1 - p_{33}}. \end{aligned} \quad (\text{D.37})$$

From the expected values for $\gamma_{\mathbf{3}}$ for all cells, the MU selects the cell which provides the minimum holding time at the failed state. Furthermore, if two or more cells have exactly the same value for π_1 , $E[\gamma_{\mathbf{3}}]$, or p_{23} , no reliability based handover will take place. Tab. D.6 summarizes the primary selection conditions of these strategies and the selected cell at the intersection based on the network scenario shown in Fig. D.1.

D.5 Obtained Per-user Availability and Discussions

Consider a region of interest as a unit area $(x_{tot}, y_{tot}) = (1, 1)$ within which an MU is moving according to the two mobility patterns discussed in Sec. D.3. In order to obtain per-user availability for a multi-cell scenario as defined in (D.36), we need to calculate the t_{in} duration inside each cell for all cells that the MU traverses through. It is obtained through simulations as follows.

Table D.6: Cell selection for 3 strategies at intersection. In this table, $p_{23}(j)$, $j = 1, 2, \dots, M$ denotes the transition probability from the occupied state to the failed state of cell j

Strategy	Main criterion for cell association	Selected cell at intersection, Cell C_s
Str_1	Steady state probability of the idle state	$C_s = \underset{j}{\operatorname{argmax}} \pi_1(j)$
Str_2	State holding time of the failed state	$C_s = \underset{j}{\operatorname{argmin}} E[\gamma_{\mathbf{3}}(j)]$
Str_3	Occupied-to-failed transition probability	$C_s = \underset{j}{\operatorname{argmin}} p_{23}(j)$

Observe the movement of the MU at a pre-defined discrete time interval t_{step} . The MU evaluates whether or not its position is inside the coverage area of a cell or multiple cells. If it is inside a single cell, its associated duration to that cell t_{in} will be incremented by t_{step} . If it is covered by two or more cells, the MU needs to select a cell to associate with according to one of the cell selection strategies presented above and obtain t_{in} in that cell accordingly. This process will continue until the MU has reached its destination or the observation duration has elapsed.

The simulation results shown below are the average values obtained based on multiple typologies for a 10-cell PV network. The state transition probabilities were selected randomly based on uniform distribution with two sets of ranges, marked as rng_1 and rng_2 respectively, as shown in Tab. D.7. These ranges are selected to reflect various channel conditions. For instance, a failed channel's recovery probability in rng_2 exhibits a larger value than that of rng_1 , leading to higher channel availability when rng_2 is adopted.

D.5.1 Multi-cell Scenario with MP1

Consider a heterogeneous network with cell sizes configured as $r = 0.3$ and $r = 0.4$ respectively. The MU traverses from $(0, 0)$ to (x_{tot}, y_{tot}) according to MP1, at a constant speed of $s = 0.01$ distance per unit time and with a given angle of departure, θ , for each journey. Fig. D.3 illustrates the availability results obtained based on the transition probabilities mentioned in rng_2 of Tab. D.7, as the angle of departure varies. Clearly, the obtained availability considering only the CR is always higher than that of the UR since the presence of RIs degrades availability. For per-user availability with RIs, Str_1 generally provides higher mean availability compared with Str_2 and Str_3 . This is because Str_1 directly relates channel availability with per-user availability as defined in (D.36). When comparing Str_2 and Str_3 , the former one performs better or equally well. This is because Str_2 focuses on minimizing the time spent in the failed state and the channel has a higher probability to return to the idle state from a failed state. Despite the fact that Str_1 performs best, Str_2 or Str_3 may be employed since they provide greater flexibility to users for faster channel recovery or for protection of ongoing traffic. Furthermore, higher availability is achieved when the angle of departure is not too close to the x- or y-axis since there is a high probability that the MU will be covered by the CR when it travels closer to the center of the region of interest.

Table D.7: Two configuration sets of transition probability ranges

	p_{12}	p_{21}	$p_{23} = p_{13}$	p_{31}
rng_1	(0.1 ~ 0.2)	(0.8 ~ 0.9)	(0.0002 ~ 0.0005)	(0.8 ~ 0.9)
rng_2	(0.01 ~ 0.1)	(0.9 ~ 0.99)	(0.0002 ~ 0.0005)	(0.9 ~ 0.99)

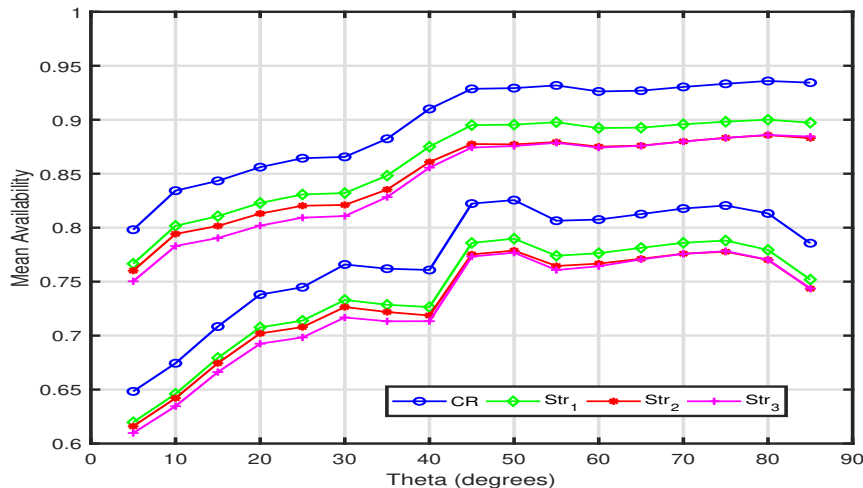


Figure D.3: Mean per-user availability in a 10-cell network with MP1. CR indicates the availability when only the coverage region is considered.

D.5.2 Multi-cell Scenario with MP2

In this case, the MU starts its journey from $(0, 0)$ and traverses through the area according to MP2 until the simulation time ends. The direction and the travel time for each phase of the journey are randomly selected from $(0.1, 0.5)$ time units and $(-\pi, \pi)$ radian ranges respectively. The travel speeds are configured from two ranges, i.e., $s_{high} \in (0.1 \sim 0.15)$ and $s_{low} \in (0.05 \sim 0.1)$ per unit time.

Fig. D.4 illustrates the average availability values obtained from multiple randomly selected trajectories according to the aforementioned configurations. The x-axis in this figure represents the speed and transition probability range combinations. From the results, it can be observed that the transition probabilities related to rng_2 provide higher availability compared with rng_1 . Having lower p_{12} values with higher p_{21} and p_{31} values results in higher channel access opportunities for new users. Moreover, a lower speed gives higher availability. This is because MU traveling at a higher speed will traverse across the CR more quickly and stay at the boundaries of a region for a longer period of time. As the network coverage is comparatively poor near the boundaries, the obtained availability becomes lower. Finally, the impact of cell selection strategies is similar to what is observed in the MP1 case.

D.5.3 Further Discussions on Availability in URC/URLLC

D.5.3.1 Availability with RIs

Overall the obtained availability levels presented in this study are generally lower than what is regarded as the URC level in the literature [2] [3]. This is because most prior work on URC/URLLC is performed based on an implicit assumption that MUs are always covered. In this study, we consider that an MU may be located outside the CR boundary for our per-user availability definition. Therefore, the proposed definition (D.35) provides a more generic and accurate metric for evaluating anytime and anywhere communication *quantitatively*, since no assumption on the availability of coverage is made herein.

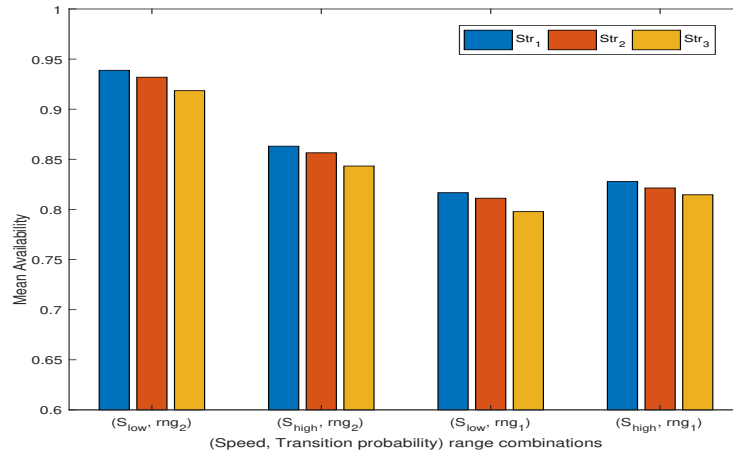


Figure D.4: Mean availability for an MU in a 10-cell network with MP2.

D.5.3.2 Shortest path versus highest availability path

Another interesting scenario to apply the proposed metric is to consider the highest availability route for user mobility. Instead of taking the shortest path towards a destination, an MU could select the path which gives the highest availability in order to satisfy its service requirements for ultra-reliable communication.

D.6 Conclusions and Future Work

This letter presents a time-space domain per-user availability analysis in 5G networks when reliability impairments are taken into consideration. We demonstrate that higher availability could be achieved by designing a proper strategy to compensate the negative effect of RIs on availability. For future work, we plan to enrich our analysis by including different RIs based on real-life measurements.

References

- [1] G. Pocovi, H. Shariatmadari, G. Berardinelli, K. Pedersen, J. Steiner, and Z. Li, “Achieving ultra-reliable low-latency communications: Challenges and envisioned system enhancements,” *IEEE Netw.*, vol. 32, no. 2, pp. 8–15, Apr. 2018.
- [2] 3GPP TR38.824, “Study on physical layer enhancements for NR ultra-reliable low latency communication (URLLC),” R16, v0.0.1, Oct. 2018.
- [3] H. V. K. Mendis and F. Y. Li, “Achieving ultra reliable communication in 5G networks: A dependability perspective availability analysis in the space domain,” *IEEE Commun. Lett.*, vol. 21, no. 9, pp. 2057–2060, Sep. 2017.
- [4] T. N. Weerasinghe, I. A. M. Balapuwaduge, and F. Y. Li, “Per-user availability for ultra-reliable communication in 5G: Concept and analysis,” in *Proc. IEEE WCNC*, Apr. 2018, pp. 1–6.

- [5] K. Marashi, S. S. Sarvestani, and A. R. Hurson, "Consideration of cyber-physical interdependencies in reliability modeling of smart grids," *IEEE Trans. Sustain. Comput.*, vol. 3, no. 2, pp. 73–83, Apr.-Jun. 2018.
- [6] C.-H. Liu and L.-C. Wang, "Random cell association and void probability in Poisson-distributed cellular networks," in *Proc. IEEE ICC*, Jun. 2015, pp. 2816–2821.
- [7] M. Garetto and E. Leonardi, "Analysis of random mobility models with partial differential equations," *IEEE Trans. Mobile Computing*, vol. 6, no. 11, pp. 1204–1217, Nov. 2007.
- [8] B. Ku, Y. Ren, J. Weng, J. Chen, and W. Chen, "Modeling and analysis of channel holding time and handoff rate for packet sessions in all-IP cellular networks," *IEEE Trans. Veh. Technol.*, vol. 66, no. 4, pp. 3331–3344, Apr. 2017.
- [9] J. Long, M. Dong, K. Ota, A. Liu, and S. Hai, "Reliability guaranteed efficient data gathering in wireless sensor networks," *IEEE Access*, vol. 3, pp. 430–444, Apr. 2015.